

Distribution Matching Distillation Meets Reinforcement Learning

Dengyang Jiang^{1,2,3} Dongyang Liu^{6,2} Zanyi Wang⁶ Qilong Wu² Liuzhuozheng Li¹ Hengzhuang Li¹ Xin Jin² David Liu^{6,2} Zhen Li² Bo Zhang⁴ Mengmeng Wang⁵ Steven Hoi² Peng Gao^{2,3*} Harry Yang^{1*}

¹The Hong Kong University of Science and Technology ²Alibaba Group ³Shenzhen Institutes of Advanced Technology

⁴Shanghai AI Laboratory ⁵Zhejiang University of Technology ⁶The Chinese University of Hong Kong

Code: <https://github.com/vvvvvjdy/dmdr>



Figure 1. **Images generated by Z-Image-Turbo [49] distilled through our DMDR.** Demonstrating excellent generation quality, ultra-realistic, outstanding concept understanding, and remarkable text rendering.

Abstract

*Distribution Matching Distillation (DMD) distills a pre-trained multi-step diffusion model to a few-step one to improve inference efficiency. However, the performance of the latter is often capped by the former. To circumvent this dilemma, we propose **DMDR**, a novel framework that combines Reinforcement Learning (RL) techniques into the distillation process. We show that for the RL of the few-step generator, the DMD loss itself is a more effective regularization compared to the traditional ones. In turn, RL can help to guide the mode coverage process in DMD more effectively. These allow us to unlock the capacity of the few-step generator by conducting distillation and RL simultaneously.*

neously. Meanwhile, we design the dynamic distribution guidance and dynamic renoise sampling training strategies to improve the initial distillation process. The experiments demonstrate that DMDR can achieve leading visual quality, prompt coherence among few-step methods, and even exhibit performance that exceeds the multi-step teacher.

1. Introduction

Diffusion models have achieved unparalleled quality in visual generation tasks [11, 21, 36, 37, 39]. Yet their sampling process typically demands tens of iterative denoising steps, each involving a full forward pass through a large neural network, which makes high-resolution text-to-image synthesis costly both in time and computation.

*Corresponding authors

To accelerate sampling speed, a surge of work [5, 31, 33, 40, 59, 60] has sought to distill the original diffusion model into a generator that needs only a handful of steps (e.g., 4). These approaches can be roughly divided into two types: distillation from the trajectory and distillation from the distribution. The former method operates on the instance level, aiming to simulate the original teacher diffusion generation trajectories in as few steps as possible [6, 31]. While the latter works at the distribution level, striving to match the output distribution of the few-step student generator to the original multi-step one’s [33, 60].

In this study, we focus on distribution matching distillation (DMD) as it has been verified in large-scale settings [28, 59] and has already been used in some leading products (e.g., Seedream 4.0 [46]). However, one notable thing is that in DMD, the student model aims to match the distribution of the teacher model, which also means that the ability of the student model is often limited by the teacher. To remedy this, most works (e.g., DMD2 [59]) introduce an additional GAN branch for guidance [16]. However, training with GAN not only renders the training process dependent on external high-quality visual data, but also introduces training instability inherent in GAN [2, 42].

To this end, we propose DMDR, which combines distribution matching distillation (DMD) with recent powerful diffusion reinforcement learning (RL) [4, 26, 50, 55]. In a nutshell, DMDR enables the student model to obtain supervision signals beyond the teacher model without relying on external image data, and makes it possible for the student to surpass the teacher. Contrary to the prevailing belief that RL should be conducted after obtaining the few-step generator, we perform RL concurrently with the distillation process. We show that such a combination is mutually beneficial: (1) As for DMD, RL can help to reshape some existing low-probability modes by guiding them toward higher reward regions, ensuring these modes are covered during the distillation process, thereby mitigating the risk of zero forcing. (2) As for RL, DMD loss itself can serve as a more effective regularization than its traditional counterparts, thereby mitigating the risk of reward hacking.

Meanwhile, since obtaining valid reward scores requires the few-step model to possess a basic generation capability already, we design two dynamic training strategies to facilitate a faster and better “cold start” for DMDR: (1) DynaDG, which strengthens the initial distributional overlap between the teacher and student model; (2) DynaRS, which enhances the student’s global modeling of the teacher’s distribution during the early training phase.

Taken together, our experimental results show that our method leads to state-of-the-art few-step generative models that can outperform their teacher, using as few as 4 sampling steps. Moreover, our method is not only compatible with different models (e.g., flow-based, denoising-based)

but also with various RL algorithms (e.g., ReFL, DPO, GRPO). This ensures the long-term effectiveness of our method as the multi-step model and RL algorithm evolve.

In summary, our main contributions are as follows:

- We propose DMDR, which shows that DMD and RL can be trained simultaneously with mutual benefits.
- We design a dynamic cold start stage for faster and better distillation in the initial phase.
- We validate our method on various models and RL algorithms with all of which achieve excellent performance.

2. Related Work

We highlight key related studies here, and leave the discussions of others in Appendix A.

Distribution Matching Distillation. Distribution Matching Distillation (DMD) [60] is the first work to successfully apply the principle score-based distillation [38, 48, 51] to large-scale text-to-image models. Intuitively, it strives to ensure that any sample realized by the student at a given noise level occurs with exactly the same probability as it would under the teacher’s distribution, thereby preserving the multi-step generative priors in the few-step model. From then on, a lot of follow-up work emerged [3, 28, 34, 56, 59], for example, DMD2 [59] employs a discriminator to align the student model distribution with a specific target distribution like GAN [16] does; TDM [34] incorporates DMD loss in the sampling process of the student model for better alignment; f -distill [56] replaces the original reverse Kullback–Leibler (KL) divergence to the proposed f -divergence for covering different divergences with different properties. Our work also starts with DMD, but we don’t focus on how to better “imitate” the teacher. Instead, we aim to incorporate reinforcement learning in the distillation process to enable the student to outperform the teacher.

Reinforce Learning for Diffusion Models. Reinforce learning helps to align diffusion models to human preferences by training a reward model and using it to guide generation [4, 26, 47, 50, 55, 57]. There are many algorithms to conduct RL, for example, DDPO [4] adapts PPO via image log-likelihoods; ReFL [55] bypasses likelihoods by optimizing outputs with frozen-reward gradients; Diffusion-DPO [50] adapts DPO to diffusion for paired human preference data; and recent GRPO extensions [26, 57] use GRPO to diffusion models by coupling the training loss with SDE samplers. Although significant progress has been made in RL for diffusion models, most of the work has focused on multi-step models. Here, we find that these algorithms are also adapted to the few-step model when carried out in conjunction with distribution matching distillation.



Figure 2. More Images generated by Z-Image-Turbo [49] distilled through our DMDR.

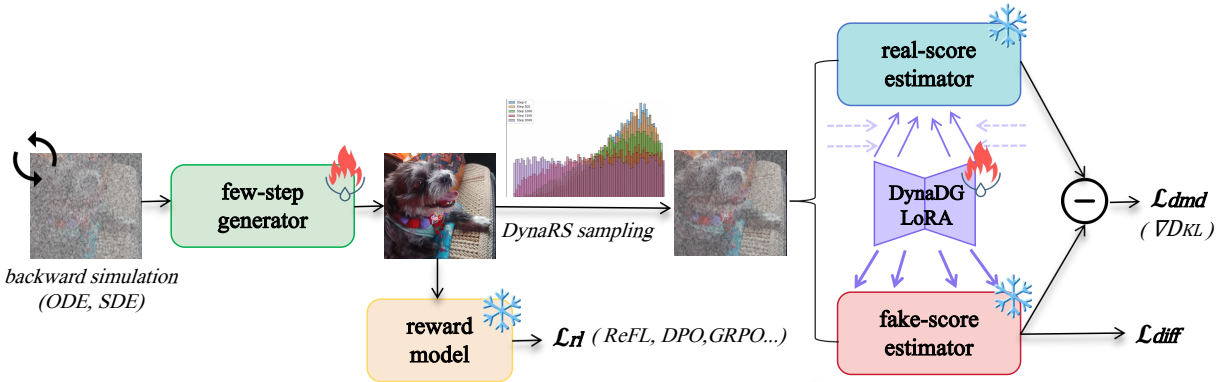


Figure 3. **Overview of DMDR**, which contains three key elements: (1) A DMD framework to optimize the generator by utilizing the gradient derived from an implicit distribution matching objective; (2) A RL branch to concurrently incorporate reward feedback from the reward model; (3) Two dynamic training strategies to facilitate more efficient and effective distillation during the initial phase.

3. Method

The pipeline of DMDR is shown in Figure 3, which contains three key elements: A DMD branch to optimize the generator using the gradient of an implicit distribution matching objective (Section 3.1); A RL branch to synchronously introduce the reward feedback from the reward model (Section 3.2); Two dynamic training strategies to achieve faster and better distillation in the initial phase (Section 3.3).

3.1. Preliminary

As our goal is to obtain a few-step model with performance beyond its multi-step teacher, and our method is built upon DMD. Here we provide a brief introduction to DMD:

Distribution Matching Distillation (DMD) [60] compresses a multi-step diffusion model (teacher) into a few-step generator (student) G by minimizing the time-averaged approximate Kullback-Leibler (KL) divergence between the real distribution $p_{\text{real},t}$ and the synthetic distribution $p_{\text{fake},t}$. Note that G is optimized via gradient descent, and this gradient admits a compact expression as the difference of two score functions:

$$\begin{aligned} \nabla_{\theta} \mathcal{L}_{\text{dmd}} &= \mathbb{E}_t [\nabla_{\theta} \text{KL}(p_{\text{fake},t} \| p_{\text{real},t})] \\ &= -\mathbb{E}_t \left[\int (s_{\text{real}}(F_t) - s_{\text{fake}}(F_t)) \frac{dG_{\theta}(z)}{d\theta} dz \right], \end{aligned} \quad (1)$$

where $z \sim \mathcal{N}(0, \mathbf{I})$, θ denotes the parameters of G , and F_t is the forward diffusion operator that injects noise at time t to $G_{\theta}(z)$. The quantities s_{real} and s_{fake} are the score functions estimated by diffusion models μ_{real} and μ_{fake} , respectively. During training, the μ_{fake} is updated via diffusion loss $\mathcal{L}_{\text{diff}}$ (for denoising-based models, the prediction target is noise, while for flow-based ones, it is velocity) on synthetic samples produced by the few-step generator. Moreover, as introduced in DMD2 [59], $G_{\theta}(z)$ is a noisy synthetic image produced by the current G running several steps, which is called backward simulation. The generator

G then denoises these simulated images, and the outputs are supervised with the above loss functions.

3.2. DMDR: Brings RL into DMD

It is worth noting that in DMD, the goal of the student generator is to align the output distribution as closely as possible with the distribution learned by the multi-step teacher. However, this also causes the ability of the student model to be capped by the teacher. Unlike the previous methods [58, 59] that introduce external real data to remedy this, we address the problem in an image-free manner by introducing the recently popular diffusion RL [26, 50, 55] in the DMD pipeline. Below, we explain how DMD and RL benefit from each other when training together.

RL Unlocks the Performance of DMD. One limitation of DMD is that the student model’s performance is inherently capped by the teacher model. By incorporating an RL objective, we allow the student model to receive supervision signals beyond merely mimicking the teacher, thus making it possible to surpass the teacher in an image-free training setup. Specifically, we integrate the reward models which

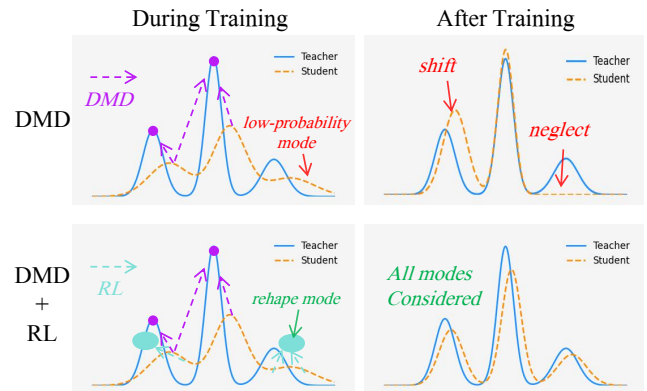


Figure 4. Illustration for mode seeking process.

provide reward signals indicating the specific characteristic

(e.g., quality, text-alignment) of a generated image. During the joint training process, the RL component guides the student generator G to produce samples that maximize these rewards. This has a direct impact on the DMD process: (1). Helping to jump out of the bad modes: The teacher’s distribution might contain modes that are less desirable or have lower perceived quality according to the reward model. RL actively discourages the student from generating samples within these low-reward regions, and “pulls” the student’s distribution towards regions in the image space that yield higher reward scores even if they are present in the teacher’s distribution. (2) Helping to mitigate zero forcing: In DMD, there’s a risk of “zero forcing,” where the student might fail to cover certain modes present in the teacher’s distribution, as we show the first row of Figure 4. By actively guiding the student towards high-reward modes, RL helps ensure that these important and preferred modes are reshaped, thus adequately covered during distillation, preventing their accidental omission as shown in the second row of Figure 4.

DMD Can Effectively Regularize RL. In addition to maximizing rewards, another important point in RL is the regularization, which helps to avoid rapid overfitting of the reward (reward hacking). Although this regularization takes on different forms in various methods (e.g., pretrain loss in ReFL [55], KL divergence loss in Flow-GRPO [26]), essentially, they all aim to let the training model be close to the reference model (always the one before RL). In the multi-step model, this is tractable because there is a pre-trained reference model. But in the few-step model, the situation is somewhat different. As shown in Figure 5, when RL is naively performed after distillation, the goal of regularization becomes to close the new model’s distribution P_{fake_new} to the distilled few-step model’s P_{fake_ref} . However, as mentioned above, some modes are inevitably neglected after being distilled, thus P_{fake_ref} cannot serve as an effective regular expression, as discovered by other works [40] that these lead to quick hacking. However, if RL and DMD are carried out simultaneously, this problem will be easily solved. The DMD loss (Equation 1) continuously pulls the student generator’s distribution (P_{fake}) towards the multi-step teacher’s distribution (P_{real}). If viewed from the RL side, this also means that at every step of the joint training, the student is being regularized by the comprehensive and robust P_{real} itself (the solid arrow “DMD + RL” in Figure 5), which reduces error accumulation in regularization and the risk of the reward hacking (see Figure 10).

Putting together, the final loss function can be written as:

$$\mathcal{L} = \mathcal{L}_{dmd} + \mathcal{L}_{rl}, \quad (2)$$

where \mathcal{L}_{rl} is the plug-and-play loss from the RL branch, the gradient can be differentiable type like ReFL, or policy type like GRPO, etc. In practice, we will multiply a coefficient if the two losses are not on the same scale.

3.3. A Dynamic Cold Start Stage for DMDR

While DMDR enables the student to surpass its teacher, the reward model often requires the generator to possess a basic generation capability to produce valid rewards [47, 55]. In practice, we observe that reward signals are noisy and unreliable in the early training phase. To this end, we conduct a cold start phase and design two dynamic training strategies based on vanilla DMD to accelerate and improve it.

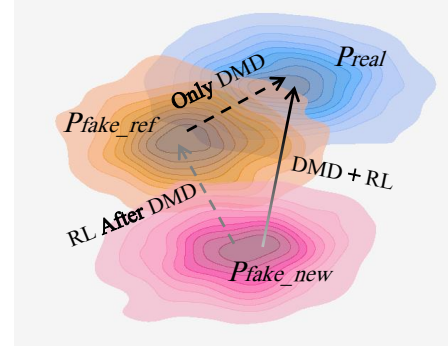


Figure 5. Visualization of distribution matching directions.

Dynamic Distribution Guidance (DynaDG). In the initial stage of training, due to the significant disparity in image quality (the generator is unable to generate qualified images), the distribution of these generated samples (P_{fake}) is completely different from that of the training samples of the real score estimator (P_{real}), which finally leads to the inaccuracies in the KL divergence approximation as we show in Figure 7 (left). This substantial divergence comes from sparse or non-existent overlap between P_{real} and P_{fake} , rendering the gradient $\nabla \log P_{real} - \nabla \log P_{fake}$ unreliable for effective optimization. Inspired by a recent study [58], we introduce a LoRA set [18] and inject it not only into the fake score estimator to learn the rapidly evolving distribution of the few-step generator but also strategically into the real score estimator. The core idea behind our DynaDG is to dynamically adjust the distribution estimated in the real score branch. By injecting LoRA into the real score estimator with a smaller scale, we can effectively “pull” the perceived P_{real} towards the nascent P_{fake} distribution, creating a region of “more overlap” as depicted in Figure 7 (right). This increased overlap ensures that the estimated score difference, $\nabla \log P_{real} - \nabla \log P_{fake}$, consistently provides a “right direction estimation and optimization” signal, even when the distributions are initially far apart. Crucially, this LoRA scale for the real score estimator gradually weakens as training progresses. This mechanism allows the real score estimator to progressively revert to accurately representing the true P_{real} as the generator improves and P_{fake} naturally converges towards P_{real} .

Dynamic Renoise Sampling (DynaRS). Another impor-

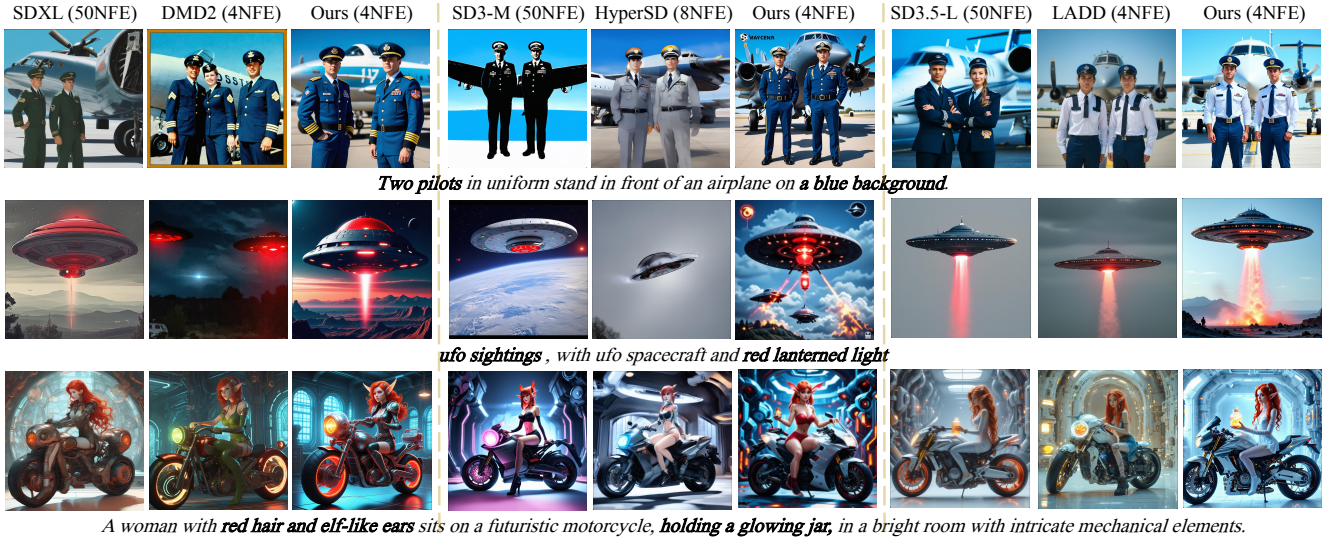


Figure 6. Visual comparison between the teachers, selected competing methods [40, 43, 59], and ours. All images are generated using identical noise. Our model produces images with superior quality and prompt coherence. More comparisons are available in Appendix B.

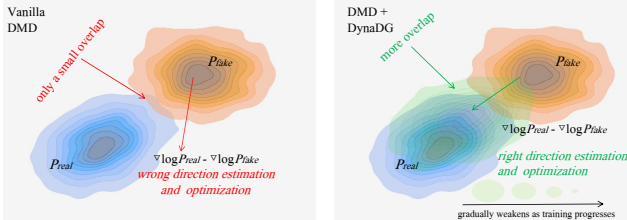


Figure 7. Illustration for our Dynamic Distribution Guidance.

tant operation in DMD is renoising, which renoises the samples generated by the generator for estimating the score (i.e., the distribution) associated with the specific noise level. The core idea of our DynaRS is to initially bias the sampling of renoise levels t in F_t towards higher values, and then gradually transition to a uniform sampling like DMD dose. This has two advantages for a faster and better cold start. First, when biasing to high noise, the forward operator makes noise largely occupy the image, so even bad samples produced by the generator in the initial stage lie in a similar regime for both real and fake estimators, thus improving score reliability and overlap. Second, the estimated score at a higher noise level is more about global structure [62, 63], which can guide the generator to first capture global structure. As the capacity of the generator improves, the renoise bias is progressively reduced, allowing the model to learn finer details by sampling from a wider range of noise levels.

3.4. Distinction from Prior Few-step RL Works

Some prior works also try to introduce RL for the few-step diffusion model [12, 29, 40, 43], but they mainly perform it after the distillation, and the problem mentioned by HyperSD [40] of quickly deviating from the original domain still

occurs. In this work, we illustrate the rationale for conducting the two simultaneously and how DMD loss can effectively regularize RL to mitigate the above problems. Meanwhile, although pioneer work like Diff-Instruct ++ [32] also introduces RL in the distillation process, our motivation and analysis are distinct, with more intuitive illustrations of the mutual benefits of the two, the verification of different diffusion models and RL algorithms at a large scale, as well as the dynamic cold start stage before incorporating RL.

4. Experiments

4.1. Experimental Setup

We provide a brief overview of our training and evaluation schemes here.

For training, we adopt denoising-based model (SDXL-Base [37]) and flow-based models (SD3-Medium [11], SD3.5-Large [1]) for distillation, using prompts from t2i-2M [10]. Additionally, we use ReFL [55] with DFN-CLIP [13] and HPSv2.1 [53] as reward models by default. As for evaluation, we validate the effect of DMDR through extensive experiments. First, we use prompts sampled from a recent public dataset ShareGPT-4o-Image [7] to generate images and follow previous work [28, 34] that report CLIP Score [17], Aesthetic Score [45], Pick Score [20], and Human Preference (HP) Score [53]. Next, in order to obtain a more comprehensive evaluation, we also compare our distilled models with their teachers on two popular benchmarks, DPG_Bench [19] and GenEval [15]. Finally, we conduct both qualitative and quantitative ablation experiments to further verify our method’s effectiveness.

Table 1. **System-level comparison** against state-of-the-art methods. * denotes our reproduced results. Best performance is marked in **Bold**. Image-Free denotes whether the training requires external image data or data generated by the multi-step teacher.

Method	Step	NFE	CLIP Score↑	Aesthetic Score↑	Pick Score↑	HP Score↑	Image-Free
<i>SDXL-Base</i>							
Base-Model (CFG = 7.0)	25	50	34.7588	5.6480	22.1085	27.1477	-
LCM [31] (CFG = 8.0)	1	2	28.4664	5.1026	20.0603	17.6837	✗
Lightning [23]	1	1	32.0283	5.6761	21.4868	26.3615	✗
DMD2 [59]	1	1	34.3046	5.6238	21.7293	26.5986	✗
DMDR (ours)	1	1	35.4835	6.0483	22.5424	31.1442	✓
DMD2 [59]	4	4	34.5169	5.7043	22.1546	28.5655	✗
DMDR (ours)	4	4	35.2940	5.9857	22.6268	32.8678	✓
<i>SD3-Medium</i>							
Base-Model (CFG = 7.0)	25	50	34.9025	5.5942	22.1801	28.4021	-
Hyper-SD [40] (CFG = 5.0)	4	8	32.0234	5.2489	20.2831	22.4544	✗
DMD2 [59]*	4	4	33.9421	5.6137	21.7688	27.3675	✗
Flash [5]	4	4	34.2634	5.6702	21.5921	26.6542	✗
TDM [34]	4	4	34.0301	5.6250	22.0010	27.7522	✓
DMDR (ours)	4	4	34.9542	5.8462	22.3578	31.8979	✓
<i>SD3.5-Large</i>							
Base-Model (CFG = 3.5)	25	50	35.5509	5.7014	22.4856	28.8135	-
LADD [43]	4	4	35.0480	5.4514	22.2451	27.8470	✗
DMDR (ours)	4	4	35.8647	6.0284	22.8859	32.4724	✓

Table 2. **Quantitative comparison on DPG_Bench** [19] of our four-step model against its multi-step teacher.

Model	Overall	Global	Entity	Attribute	Relation	Other
<i>SDXL-Base</i>						
Teacher	74.65	83.27	82.43	80.91	86.76	80.41
Ours	76.44	83.70	82.54	83.66	84.75	83.49
<i>SD3-Medium</i>						
Teacher	84.08	87.90	91.01	88.83	80.70	88.68
Ours	84.96	90.46	90.05	90.52	87.12	91.23
<i>SD3.5-Large</i>						
Teacher	84.12	91.48	90.22	87.81	91.20	89.49
Ours	85.30	90.46	90.50	90.66	87.40	90.18

4.2. Main Results

We begin by assessing DMDR’s text-to-image generation performance using prompts sampled from ShareGPT-4-Image [7], ensuring that there is no overlap with the prompts utilized during training. Table 1 presents a summary of the distillation results in comparison to other methods. Models distilled through our approach exhibit state-of-the-art (SOTA) capabilities in terms of prompt coherence and the generation of high-quality, aesthetically pleasing images. Notably, our method demonstrates effectiveness across various architectures (e.g., UNet, Transformer), model sizes (e.g., 2B, 8B), and paradigms (e.g., flow-based, denoising-based), highlighting the broad applicability and universality of the proposed approach. Additionally, we provide qualitative comparisons in Figure 6 and Appendix B, where our method produces images characterized by superior quality and enhanced prompt coherence.

To further verify our method’s effectiveness and pro-

Table 3. **Quantitative comparison on GenEval** [15] of our four-step model against its multi-step teacher.

Model	Overall	Single	Two	Count.	Colors	Pos.	Attr.
<i>SDXL-Base</i>							
Teacher	0.55	0.98	0.74	0.39	0.85	0.15	0.23
Ours	0.56	0.99	0.76	0.42	0.84	0.11	0.24
<i>SD3-Medium</i>							
Teacher	0.62	0.98	0.74	0.63	0.67	0.34	0.36
Ours	0.64	0.99	0.84	0.54	0.81	0.25	0.44
<i>SD3.5-Large</i>							
Teacher	0.71	0.98	0.89	0.73	0.83	0.34	0.47
Ours	0.72	0.99	0.93	0.68	0.80	0.30	0.59

vide a more comprehensive comparison between the few-step distillation model and the multi-step teacher model, we conduct the comparison on two commonly used benchmarks [15, 19]. Table 2 shows our four-step model consistently outperforms its multi-step teacher on DPG_Bench across all base models, lifting the overall score from 74.65 to 76.44 for SDXL-Base, 84.08 to 84.96 for SD3-Medium, and 84.12 to 85.30 for SD3.5-Large. Meanwhile, on GenEval (Table 3) the same trend holds: overall scores improve for SDXL (0.55 → 0.56), SD3 (0.62 → 0.64), and SD3.5 (0.71 → 0.72). These results indicate that DMDR has successfully freed the student model from the constraints of the multi-step teacher model and stimulated its capabilities during the distillation process.

4.3. Ablation Study

We investigate our method’s properties below. We use SD3-Medium with 512 × 512 resolution by default for a fast ablation.

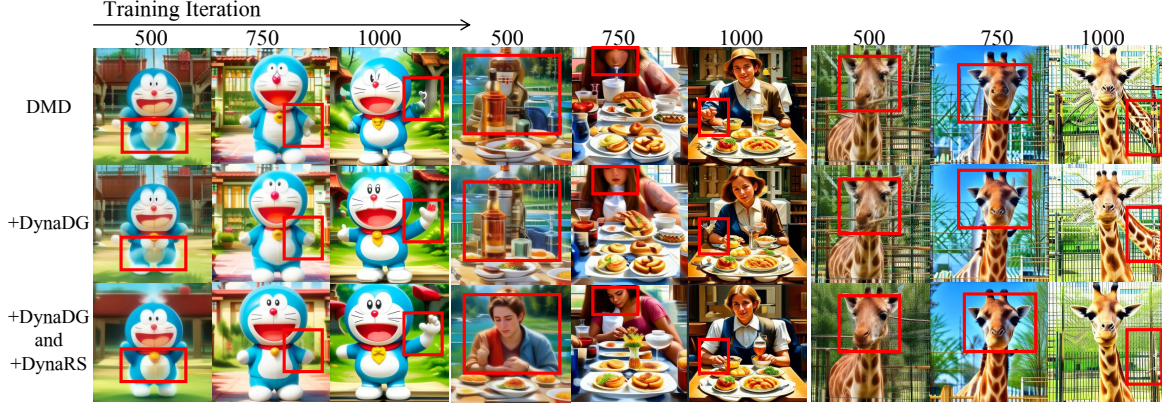


Figure 8. **Ablation examples of two dynamic training strategies.** Better to zoom in to check the effect.

Table 4. **Ablation on our dynamic cold start stage.**

Method	1000 iter		2000 iter	
	CLIP Score	HP Score	CLIP Score	HP Score
vanilla.DMD	31.5608	27.0051	32.5492	28.4541
+DynaDG	32.7905	27.5723	33.5045	29.0363
+DynaRS	33.1657	27.8276	33.6432	29.1157
-Dynamic	32.6562	27.2641	33.0245	28.8459

Effect of Dynamic Cold Start Stage. As shown in Table 4, our dynamic cold start strategies significantly enhance the initial training phase. Firstly, introducing DynaDG leads to a notable improvement. By dynamically adjusting the P_{real} to create more overlap with the nascent P_{fake} distribution, DynaDG provides more reliable gradient signals. Quantitatively, this translates to a CLIP Score increase from 31.56 to 32.79 (+1.23) and an HP Score increase from 27.01 to 27.57 (+0.56) at 1000 iterations. Similar gains are observed at 2000 iterations. Further incorporating DynaRS, which initially biases renoise sampling towards higher noise levels, guiding the generator to learn global structures before progressively shifting to finer details, further boosts performance. To highlight the importance of the dynamic aspect of our strategies, we evaluate a variant denoted as -Dynamic. This variant removes the dynamic scaling of LoRA in DynaDG (e.g., using a fixed LoRA scale) and employs biased renoise sampling in the whole training process. While it still outperforms vanilla_DMD, it consistently underperforms the full dynamic approaches. This clearly indicates that the adaptive, progressive nature of our DynaDG and DynaRS mechanisms is crucial for maximizing performance during the cold start phase. Qualitative results presented in Figure 8 further corroborate these findings, showing a faster global structure building when our dynamic cold start strategies are employed.

Effect of DMDR with Different RL Algorithms. We choose three representative RL methods [26, 50, 55] to illustrate the efficacy of combining distillation with various RL techniques in DMDR, the results are provided in Ta-

Table 5. **Ablation on RL and DMD.** We init the model after cold start for 2K iteration then continue training in different ways.

Method	CLIP Score	Aesthetic Score	Pick Score	HP Score
<i>init</i>	33.6432	5.6124	21.0489	29.1157
w/ only Distill.	33.6738	5.6248	21.6376	29.1389
w/ only RL (ReFL)	33.1897	5.8841	22.3008	31.2714
w/ Distill. + RL (ReFL)	34.6249	6.1813	22.7578	32.8979
w/ only RL (DPO)	33.9554	5.7893	21.7643	29.5819
w/ Distill. + RL (DPO)	33.9632	5.9710	21.9865	30.5994
w/ only RL (GRPO)	33.9095	5.7876	21.7956	29.4429
w/ Distill. + RL (GRPO)	34.0055	5.8256	22.0120	30.6248

ble 5. Firstly, we observe that the initial model state after our dynamic cold start stage already provides a good baseline performance. Training with “w/ only Distill.”, as we illustrated above, this would be inherently capped by the teacher’s distribution, resulting in a very minor improvement over the initial state. Next, when considering introducing different RL algorithms (the regularization originally used in these methods has also been added), although these show improvements in some metrics, they do not consistently surpass the “only Distill” baseline across all scores. Moreover, the reward hacking occurs (we will analyze it specifically in the next part). Crucially, the rows corresponding to “w/ Distill. + RL” consistently demonstrates superior performance across all evaluated metrics against the counterparts. Figure 9 also shows superior visualization results when DMD and RL are conducted together. These validate our core insight that RL unlocks the performance potential of DMD, allowing the student model to surpass the teacher’s inherent limitations by optimizing for external reward signals. Simultaneously, DMD effectively regularizes the RL process, preventing reward hacking and ensuring that the student’s distribution remains robust and comprehensive, as evidenced by the consistent improvements across diverse metrics with different RL algorithms.

Furthermore, an interesting observation is that using the



Figure 9. **Ablation examples of different RL algorithms with DMD.** Better to zoom in to check the effect.

ReFL style RL method achieves overall better performance, and our analysis is that: traditional ReFL for multi-step models ignores earlier sampling steps and only trains the last few steps before the output image [55] because the large computational graph generated by the gradient of the reward model and the multi-step denoising process would result in a huge memory consumption. Subsequent works [47, 54] mainly focus on saving forward noise trajectory and sampling a subset of steps to optimize to remedy this dilemma, although this can allow the gradient to return to the early denoising step, it is also prone to error accumulation. On the contrary, in our few-step model, the model is trained to predict a clean image at each step’s state [59], which enables the gradient of ReFL to directly return to the initial state, thus obtaining an effective optimization.

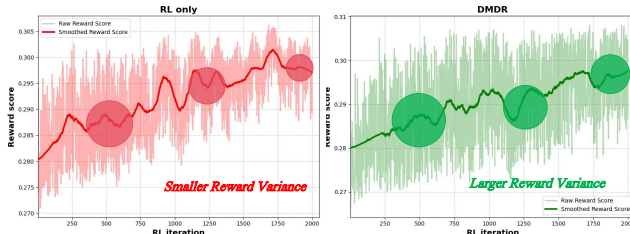


Figure 10. **Reward curves comparison** during the RL stage. Better to zoom in to check the difference.

Effect of DMDR to Mitigate Reward Hacking. We follow RewardDance [52] to present the reward curves during training illustrated in Figure 10. It is evident that employing DMD loss as a form of regularization (right) demonstrates significantly greater variance throughout the training process compared to the traditional approach (left). This increased diversity in reward signals suggests that models trained using our method exhibit enhanced robustness against reward hacking. This assertion is further supported by Figure 9, which shows that in the absence of DMD loss,

Table 6. Diversity evaluation on ShareGPT-4o-Image [7].

	DMD	DMD2	Ours	Teacher
LPIPS↑ [61]	0.5664	0.5832	0.5513	0.6480

utilizing ReFL results in a rasterized appearance of images, indicating the occurrence of reward hacking.

5. Limitation and Future Work

We discuss some limitations we realized during the development of DMDR. We hope these will serve as a catalyst for innovative ideas and advancements in future research.

Quality vs. Diversity. One notable thing is the trade-off between quality and diversity. Although models trained from our method show superior quality and prompt coherence, the diversity is reduced like shown in Table 6. We believe that this is a common feature of score distillation like DMD and RL, that is, sacrificing uncertainty in sampling in exchange for stable and desired results, not a limitation unique to our approach. The reduced diversity caused by DMD, we believe, will also have some impact on some online RL methods that require a group of samples for ranking then optimization. This is also reflected in the slightly poorer improvement of GRPO and DPO compared to ReFL in the Table 5. Further investigation into finding the optimal balance between quality and diversity is left for future work.

Scaling of Reward Model. Another notable thing is the scaling of the reward model in DMDR. Our experimental results demonstrate that our method enables the few-step model to be able to surpass its teacher model. However, as indicated in the Table 2 and 3, certain metrics exhibit a decline after the distillation. We attribute this degradation primarily to inherent limitations and potential biases present in the open-source reward model we employed. Notably, RewardDance [52] has shown that scaling up the reward model yields consistent improvements for RL in multi-step diffusion models. We posit that similar benefits would extend to

few-step models with our method, but require more computation resources, which we leave for future work.

6. Conclusion

This work introduces DMDR, which combines Distribution Matching Distillation (DMD) with reinforcement learning (RL) in one framework. We show that DMD and RL can be trained simultaneously, with RL enabling the student model to surpass the teacher and DMD loss regularizing RL to prevent reward hacking. We also propose dynamic training strategies (DynaDG and DynaRS) to enhance the initial distillation process. Experiments demonstrate state-of-the-art performance among few-step methods and overall superior performance against multi-step teachers.

References

- [1] Stability AI. Sd3.5. <https://github.com/Stability-AI/sd3.5>, 2024. 6
- [2] Martin Arjovsky and Léon Bottou. Towards principled methods for training generative adversarial networks. *arXiv preprint arXiv:1701.04862*, 2017. 2
- [3] Hmrishav Bandyopadhyay, Rahim Entezari, Jim Scott, Reshith Adithyan, Yi-Zhe Song, and Varun Jampani. Sd3.5-flash: Distribution-guided distillation of generative flows. *arXiv preprint arXiv:2509.21318*, 2025. 2
- [4] Kevin Black, Michael Janner, Yilun Du, Ilya Kostrikov, and Sergey Levine. Training diffusion models with reinforcement learning. *arXiv preprint arXiv:2305.13301*, 2023. 2
- [5] Clement Chadebec, Onur Tasar, Eyal Benaroché, and Benjamin Aubin. Flash diffusion: Accelerating any conditional diffusion model for few steps image generation. In *Proceedings of the AAAI Conference on Artificial Intelligence*, pages 15686–15695, 2025. 2, 7
- [6] Hansheng Chen, Kai Zhang, Hao Tan, Leonidas Guibas, Gordon Wetzstein, and Sai Bi. pi-flow: Policy-based few-step generation via imitation distillation. *arXiv preprint arXiv:2510.14974*, 2025. 2, 13
- [7] Junying Chen, Zhenyang Cai, Pengcheng Chen, Shunian Chen, Ke Ji, Xidong Wang, Yunjin Yang, and Benyou Wang. Sharegpt-4o-image: Aligning multimodal models with gpt-4o-level image generation. *arXiv preprint arXiv:2506.18095*, 2025. 6, 7, 9
- [8] Junsong Chen, Shuchen Xue, Yuyang Zhao, Jincheng Yu, Sayak Paul, Junyu Chen, Han Cai, Song Han, and Enze Xie. Sana-sprint: One-step diffusion with continuous-time consistency distillation. *arXiv preprint arXiv:2503.09641*, 2025. 13
- [9] Jiaxiang Cheng, Bing Ma, Xuhua Ren, Hongyi Jin, Kai Yu, Peng Zhang, Wenyue Li, Yuan Zhou, Tianxiang Zheng, and Qinglin Lu. Pose: Phased one-step adversarial equilibrium for video diffusion models. *arXiv preprint arXiv:2508.21019*, 2025. 13
- [10] Hugging Face Open Data. text-to-image-2m. <https://huggingface.co/datasets/jackyhate/text-to-image-2M>, 2024. 6
- [11] Patrick Esser, Sumith Kulal, Andreas Blattmann, Rahim Entezari, Jonas Müller, Harry Saini, Yam Levi, Dominik Lorenz, Axel Sauer, Frederic Boesel, et al. Scaling rectified flow transformers for high-resolution image synthesis. In *Forty-first international conference on machine learning*, 2024. 1, 6
- [12] Luca Eyring, Shyamgopal Karthik, Alexey Dosovitskiy, Nataniel Ruiz, and Zeynep Akata. Noise hypernetworks: Amortizing test-time compute in diffusion models. *arXiv preprint arXiv:2508.09968*, 2025. 6
- [13] Alex Fang, Albin Madappally Jose, Amit Jain, Ludwig Schmidt, Alexander Toshev, and Vaishaal Shankar. Data filtering networks. *arXiv preprint arXiv:2309.17425*, 2023. 6
- [14] Kevin Frans, Danijar Hafner, Sergey Levine, and Pieter Abbeel. One step diffusion via shortcut models. *arXiv preprint arXiv:2410.12557*, 2024. 13
- [15] Dhruba Ghosh, Hannaneh Hajishirzi, and Ludwig Schmidt. Geneval: An object-focused framework for evaluating text-to-image alignment. *Advances in Neural Information Processing Systems*, 36:52132–52152, 2023. 6, 7
- [16] Ian Goodfellow, Jean Pouget-Abadie, Mehdi Mirza, Bing Xu, David Warde-Farley, Sherjil Ozair, Aaron Courville, and Yoshua Bengio. Generative adversarial nets. *Advances in neural information processing systems*, 27, 2014. 2, 13
- [17] Jack Hessel, Ari Holtzman, Maxwell Forbes, Ronan Le Bras, and Yejin Choi. Clipscore: A reference-free evaluation metric for image captioning. *arXiv preprint arXiv:2104.08718*, 2021. 6
- [18] Edward J Hu, Yelong Shen, Phillip Wallis, Zeyuan Allen-Zhu, Yuanzhi Li, Shean Wang, Lu Wang, Weizhu Chen, et al. Lora: Low-rank adaptation of large language models. *ICLR*, 1(2):3, 2022. 5
- [19] Xiwei Hu, Rui Wang, Yixiao Fang, Bin Fu, Pei Cheng, and Gang Yu. Ella: Equip diffusion models with llm for enhanced semantic alignment. *arXiv preprint arXiv:2403.05135*, 2024. 6, 7
- [20] Yuval Kirstain, Adam Polyak, Uriel Singer, Shahbuland Maitiana, Joe Penna, and Omer Levy. Pick-a-pic: An open dataset of user preferences for text-to-image generation. *Advances in neural information processing systems*, 36:36652–36663, 2023. 6
- [21] Black Forest Labs. Flux. <https://github.com/black-forest-labs/flux>, 2024. 1
- [22] Shanchuan Lin and Xiao Yang. Animatediff-lightning: Cross-model diffusion distillation. *arXiv preprint arXiv:2403.12706*, 2024. 13
- [23] Shanchuan Lin, Anran Wang, and Xiao Yang. Sdxl-lightning: Progressive adversarial diffusion distillation. *arXiv preprint arXiv:2402.13929*, 2024. 7
- [24] Shanchuan Lin, Xin Xia, Yuxi Ren, Ceyuan Yang, Xuefeng Xiao, and Lu Jiang. Diffusion adversarial post-training for one-step video generation. *arXiv preprint arXiv:2501.08316*, 2025. 13
- [25] Shanchuan Lin, Ceyuan Yang, Hao He, Jianwen Jiang, Yuxi Ren, Xin Xia, Yang Zhao, Xuefeng Xiao, and Lu Jiang. Autoregressive adversarial post-training for real-time interactive video generation. *arXiv preprint arXiv:2506.09350*, 2025. 13

[26] Jie Liu, Gongye Liu, Jiajun Liang, Yangguang Li, Jiaheng Liu, Xintao Wang, Pengfei Wan, Di Zhang, and Wanli Ouyang. Flow-grpo: Training flow matching models via online rl. *arXiv preprint arXiv:2505.05470*, 2025. 2, 4, 5, 8

[27] Cheng Lu and Yang Song. Simplifying, stabilizing and scaling continuous-time consistency models. *arXiv preprint arXiv:2410.11081*, 2024. 13

[28] Yanzuo Lu, Yuxi Ren, Xin Xia, Shanchuan Lin, Xing Wang, Xuefeng Xiao, Andy J Ma, Xiaohua Xie, and Jian-Huang Lai. Adversarial distribution matching for diffusion distillation towards efficient image and video synthesis. *arXiv preprint arXiv:2507.18569*, 2025. 2, 6

[29] Yanzuo Lu, Xin Xia, Manlin Zhang, Huafeng Kuang, Jianbin Zheng, Yuxi Ren, and Xuefeng Xiao. Hyper-bagel: A unified acceleration framework for multimodal understanding and generation. *arXiv preprint arXiv:2509.18824*, 2025. 6

[30] Eric Luhman and Troy Luhman. Knowledge distillation in iterative generative models for improved sampling speed. *arXiv preprint arXiv:2101.02388*, 2021. 13

[31] Simian Luo, Yiqin Tan, Longbo Huang, Jian Li, and Hang Zhao. Latent consistency models: Synthesizing high-resolution images with few-step inference. *arXiv preprint arXiv:2310.04378*, 2023. 2, 7, 13

[32] Weijian Luo. Diff-instruct++: Training one-step text-to-image generator model to align with human preferences. *arXiv preprint arXiv:2410.18881*, 2024. 6

[33] Weijian Luo, Tianyang Hu, Shifeng Zhang, Jiacheng Sun, Zhenguo Li, and Zhihua Zhang. Diff-instruct: A universal approach for transferring knowledge from pre-trained diffusion models. *Advances in Neural Information Processing Systems*, 36:76525–76546, 2023. 2

[34] Yihong Luo, Tianyang Hu, Jiacheng Sun, Yujun Cai, and Jing Tang. Learning few-step diffusion models by trajectory distribution matching. *arXiv preprint arXiv:2503.06674*, 2025. 2, 6, 7, 13

[35] Lars Mescheder, Andreas Geiger, and Sebastian Nowozin. Which training methods for gans do actually converge? In *International conference on machine learning*, pages 3481–3490. PMLR, 2018. 13

[36] William Peebles and Saining Xie. Scalable diffusion models with transformers. In *Proceedings of the IEEE/CVF international conference on computer vision*, pages 4195–4205, 2023. 1

[37] Dustin Podell, Zion English, Kyle Lacey, Andreas Blattmann, Tim Dockhorn, Jonas Müller, Joe Penna, and Robin Rombach. Sdxl: Improving latent diffusion models for high-resolution image synthesis. *arXiv preprint arXiv:2307.01952*, 2023. 1, 6

[38] Ben Poole, Ajay Jain, Jonathan T Barron, and Ben Mildenhall. Dreamfusion: Text-to-3d using 2d diffusion. *arXiv preprint arXiv:2209.14988*, 2022. 2

[39] Qi Qin, Le Zhuo, Yi Xin, Ruoyi Du, Zhen Li, Bin Fu, Yiting Lu, Xinyue Li, Dongyang Liu, Xiangyang Zhu, et al. Lumina-image 2.0: A unified and efficient image generative framework. *arXiv preprint arXiv:2503.21758*, 2025. 1

[40] Yuxi Ren, Xin Xia, Yanzuo Lu, Jiacheng Zhang, Jie Wu, Pan Xie, Xing Wang, and Xuefeng Xiao. Hyper-sd: Trajectory segmented consistency model for efficient image synthesis. *arXiv preprint arXiv:2404.13686*, 2024. 2, 5, 6, 7, 13

[41] Kevin Roth, Aurelien Lucchi, Sebastian Nowozin, and Thomas Hofmann. Stabilizing training of generative adversarial networks through regularization. *Advances in neural information processing systems*, 30, 2017. 13

[42] Tim Salimans, Ian Goodfellow, Wojciech Zaremba, Vicki Cheung, Alec Radford, and Xi Chen. Improved techniques for training gans. *Advances in neural information processing systems*, 29, 2016. 2, 13

[43] Axel Sauer, Frederic Boesel, Tim Dockhorn, Andreas Blattmann, Patrick Esser, and Robin Rombach. Fast high-resolution image synthesis with latent adversarial diffusion distillation. In *SIGGRAPH Asia 2024 Conference Papers*, pages 1–11, 2024. 6, 7, 13

[44] Axel Sauer, Dominik Lorenz, Andreas Blattmann, and Robin Rombach. Adversarial diffusion distillation. In *European Conference on Computer Vision*, pages 87–103. Springer, 2024. 13

[45] Christoph Schuhmann, Romain Beaumont, Richard Vencu, Cade Gordon, Ross Wightman, Mehdi Cherti, Theo Coombes, Aarush Katta, Clayton Mullis, Mitchell Wortsman, et al. Laion-5b: An open large-scale dataset for training next generation image-text models. *Advances in neural information processing systems*, 35:25278–25294, 2022. 6

[46] Team Seedream, Yunpeng Chen, Yu Gao, Lixue Gong, Meng Guo, Qiushan Guo, Zhiyao Guo, Xiaoxia Hou, Weilin Huang, Yixuan Huang, et al. Seedream 4.0: Toward next-generation multimodal image generation. *arXiv preprint arXiv:2509.20427*, 2025. 2

[47] Xiangwei Shen, Zhimin Li, Zhantao Yang, Shiyi Zhang, Yingfang Zhang, Donghao Li, Chunyu Wang, Qinglin Lu, and Yansong Tang. Directly aligning the full diffusion trajectory with fine-grained human preference. *arXiv preprint arXiv:2509.06942*, 2025. 2, 5, 9

[48] Yang Song, Jascha Sohl-Dickstein, Diederik P Kingma, Abhishek Kumar, Stefano Ermon, and Ben Poole. Score-based generative modeling through stochastic differential equations. *arXiv preprint arXiv:2011.13456*, 2020. 2

[49] Z-Image Team. Z-image: An efficient image generation foundation model with single-stream diffusion transformer. *arXiv preprint arXiv:2511.22699*, 2025. 1, 3

[50] Bram Wallace, Meihua Dang, Rafael Rafailov, Linqi Zhou, Aaron Lou, Senthil Purushwalkam, Stefano Ermon, Caiming Xiong, Shafiq Joty, and Nikhil Naik. Diffusion model alignment using direct preference optimization. In *Proceedings of the IEEE/CVF Conference on Computer Vision and Pattern Recognition*, pages 8228–8238, 2024. 2, 4, 8

[51] Zhengyi Wang, Cheng Lu, Yikai Wang, Fan Bao, Chongxuan Li, Hang Su, and Jun Zhu. Prolificdreamer: High-fidelity and diverse text-to-3d generation with variational score distillation. *Advances in neural information processing systems*, 36: 8406–8441, 2023. 2

[52] Jie Wu, Yu Gao, Zilyu Ye, Ming Li, Liang Li, Hanzhong Guo, Jie Liu, Zeyue Xue, Xiaoxia Hou, Wei Liu, et al. Rewarddance: Reward scaling in visual generation. *arXiv preprint arXiv:2509.08826*, 2025. 9

[53] Xiaoshi Wu, Yiming Hao, Keqiang Sun, Yixiong Chen, Feng Zhu, Rui Zhao, and Hongsheng Li. Human preference score v2: A solid benchmark for evaluating human preferences of text-to-image synthesis. *arXiv preprint arXiv:2306.09341*, 2023. 6

[54] Xiaoshi Wu, Yiming Hao, Manyuan Zhang, Keqiang Sun, Zhaoyang Huang, Guanglu Song, Yu Liu, and Hongsheng Li. Deep reward supervisions for tuning text-to-image diffusion models. In *European Conference on Computer Vision*, pages 108–124. Springer, 2024. 9

[55] Jiazheng Xu, Xiao Liu, Yuchen Wu, Yuxuan Tong, Qinkai Li, Ming Ding, Jie Tang, and Yuxiao Dong. Imageward: Learning and evaluating human preferences for text-to-image generation. *Advances in Neural Information Processing Systems*, 36:15903–15935, 2023. 2, 4, 5, 6, 8, 9

[56] Yilun Xu, Weili Nie, and Arash Vahdat. One-step diffusion models with f -divergence distribution matching. *arXiv preprint arXiv:2502.15681*, 2025. 2

[57] Zeyue Xue, Jie Wu, Yu Gao, Fangyuan Kong, Lingting Zhu, Mengzhao Chen, Zhiheng Liu, Wei Liu, Qishan Guo, Weilin Huang, et al. Dancegrpo: Unleashing grp on visual generation. *arXiv preprint arXiv:2505.07818*, 2025. 2

[58] Hongwei Yi, Shitong Shao, Tian Ye, Jiantong Zhao, Qingyu Yin, Michael Lingelbach, Li Yuan, Yonghong Tian, Enze Xie, and Daquan Zhou. Magic 1-for-1: Generating one minute video clips within one minute. *arXiv preprint arXiv:2502.07701*, 2025. 4, 5

[59] Tianwei Yin, Michaël Gharbi, Taesung Park, Richard Zhang, Eli Shechtman, Fredo Durand, and Bill Freeman. Improved distribution matching distillation for fast image synthesis. *Advances in neural information processing systems*, 37:47455–47487, 2024. 2, 4, 6, 7, 9

[60] Tianwei Yin, Michaël Gharbi, Richard Zhang, Eli Shechtman, Fredo Durand, William T Freeman, and Taesung Park. One-step diffusion with distribution matching distillation. In *Proceedings of the IEEE/CVF conference on computer vision and pattern recognition*, pages 6613–6623, 2024. 2, 4, 13

[61] Richard Zhang, Phillip Isola, Alexei A Efros, Eli Shechtman, and Oliver Wang. The unreasonable effectiveness of deep features as a perceptual metric. In *Proceedings of the IEEE conference on computer vision and pattern recognition*, pages 586–595, 2018. 9

[62] Yuxin Zhang, Weiming Dong, Fan Tang, Nisha Huang, Haibin Huang, Chongyang Ma, Tong-Yee Lee, Oliver Deussen, and Changsheng Xu. Prospect: Prompt spectrum for attribute-aware personalization of diffusion models. *ACM Transactions on Graphics (TOG)*, 42(6):1–14, 2023. 6

[63] Zhanjie Zhang, Quanwei Zhang, Huaizhong Lin, Wei Xing, Juncheng Mo, Shuaicheng Huang, Jinheng Xie, Guangyuan Li, Junsheng Luan, Lei Zhao, et al. Towards highly realistic artistic style transfer via stable diffusion with step-aware and layer-aware prompt. *arXiv preprint arXiv:2404.11474*, 2024. 6

[64] Kaiwen Zheng, Yuji Wang, Qianli Ma, Huayu Chen, Jintao Zhang, Yogesh Balaji, Jianfei Chen, Ming-Yu Liu, Jun Zhu, and Qinsheng Zhang. Large scale diffusion distillation via score-regularized continuous-time consistency. *arXiv preprint arXiv:2510.08431*, 2025. 13

Appendix

A. More Related Works

Trajectory-Based Distillation. Trajectory-based distillation [6, 31, 40, 64], which typically aims to simulate teacher ODE trajectories on the instance level. Early work [30] regresses the teacher’s ODE integral in one step, producing blurry ℓ_2 - x_0 estimates, and thus suffers from degraded quality. Progressive distillation [14, 40] mitigates this by a multi-stage pipeline that enlarges the student’s step size and halves its NFE each stage by distilling the prior stage’s trajectory into fewer steps. However, this not only makes the training a multi-stage process (e.g., NFE from 50 to 25 then to 10, etc.), but also leads to cumulative errors. Meanwhile, consistency models [27, 31] aim to learn a consistency function that maps the point at an arbitrary time t on the teacher’s PF-ODE trajectory to the initial point. However, the student model must be constructed implicitly using either inaccurate finite differences or expensive Jacobian–vector products (JVPs) and the quality is still limited due to the accumulation of errors into the integrated state, which limits the application in large-scale scenarios [6, 64].

Adversarial Distillation. Adversarial distillation [24, 25, 43, 44] can be regarded as another form of distribution matching distillation. The difference is that adversarial distillation aim to estimate the distribution of both the student model and the real data or the teacher model through a discriminator model [16] to match the distribution. Representative works like Adversarial Diffusion Distillation (ADD) [44] force the few-step student diffusion model to fool a discriminator which is trained to distinguish the generated samples from real images. Follow-up works [24, 25] applied this idea to other fields. However, such a training method can cause many instabilities, similar to traditional GANs [16, 42], hence requires a lot of tricks to stabilize training [22, 35, 41].

Other Distillation Works. Other distillation works mainly focus on combining the distillation at the distribution level and the trajectory level [8, 9, 34, 64]. For example, SANA-Sprint [8] combines the ideas of LADD [43] and sCM [27] and achieves fast convergence and high fidelity generation while retaining the alignment advantages of sCMs. TDM [34] and rCM [64] combine DMD [60] and LCM [31] together to remedy the quality issues of LCM.

B. Additional Visual Comparison Results

In this section, we provide additional visual comparisons for our 4-step distilled models against teacher models and other methods. The results are shown in Figure 11, Figure 12:

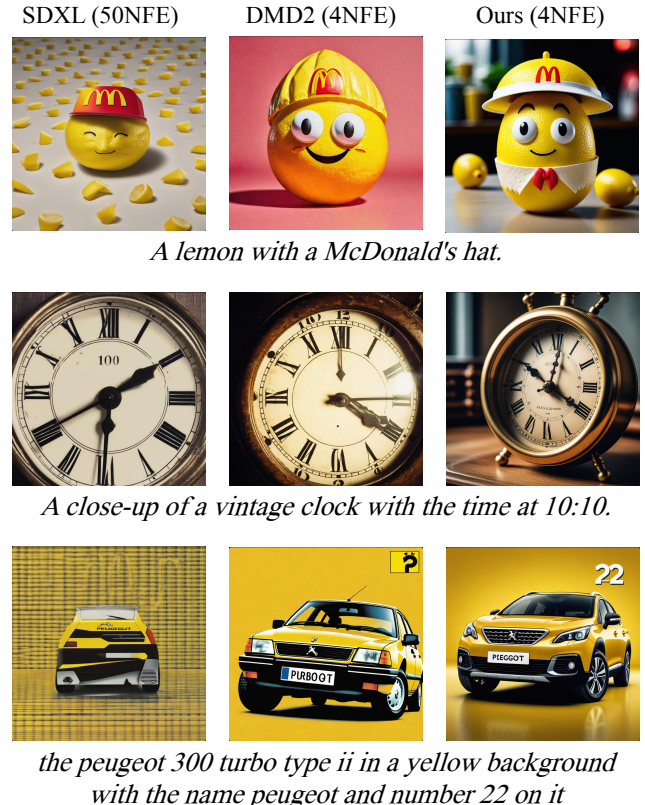


Figure 11. Additional visual comparison in SDXL-Base. All images are generated using identical noise and text prompts. Our model produces images with superior quality and prompt coherence.



a snap back new york yankees cap



new balance 997 hook - strap, bright pink with grey



In a fiery landscape, a heavily armored figure wields a dual-purpose weapon: an axe at one end and a spiked orb at the other, while clad in golden armor covering his upper body.

Figure 12. Additional visual comparison in SD3-Medium. All images are generated using identical noise and text prompts. Our model produces images with superior quality and prompt coherence.



Vibrant urban alley with a graffiti wall prominently spray-painted 'Street Art Rules', surrounded by colorful tags and murals, under a sunny sky



mane mane with money bag mini button



A modern entertainment center with a flat-screen TV, gaming console, and audio equipment.

Figure 13. Additional visual comparison in SD3.5-Large. All images are generated using identical noise and text prompts. Our model produces images with superior quality and prompt coherence.